

The Interaction Between Transport and Reconnection Processes

H.R. Wilson 1), D.J. Applegate 2), J.W. Connor 2) and M. James 2,3)

1) Department of Physics, University of York, Heslington, York YO10 5DD UK

2) EURATOM/UKAEA Fusion Association, Culham Science Centre, Abingdon, Oxon OX14 3DB, UK

3) University of Bristol, Senate House, Tyndall Avenue, Bristol BS8 1TH UK

e-mail contact of main author: hw508@york.ac.uk

Abstract. The interaction between transport and reconnection processes in magnetically confined plasmas is discussed. There are two complementary processes that we describe. In the first, we consider magnetic islands in a slab geometry to explore the impact of the magnetic island on ion temperature gradient stability. A local theory demonstrates a strong stabilising influence as a consequence of the suppression of gradients within the island. However, a non-local theory predicts that the presence of the magnetic island permits instabilities with a new mode structure that can be unstable. The second process addresses the impact of transport processes on the rate of reconnection. Specifically, we calculate the plasma density and flow profiles in the vicinity of the island in the situation when free streaming along magnetic field lines dominates over diffusion processes. This approximation is valid everywhere except in a narrow layer near the island separatrix, where cross-field diffusion competes with parallel free streaming. A solution in this layer is presented and matched to the solution in the external region through an intermediate collisional matching region.

1. Introduction

Tearing modes are generally believed to be detrimental to the fusion performance of tokamaks and, in particular, neoclassical tearing modes (NTMs) on ITER are a significant issue. In this paper we address two issues associated with the transport physics of tearing modes in magnetically confined plasmas. Large magnetic islands lead to a flattening of the pressure profile in their vicinity and, therefore, clearly degrade the confinement. However, in the case of small, isolated magnetic islands, the situation is less clear. First, the pressure is flattened over a small region, so this effect is not great. Second, the effect of the island on the pressure and flow profiles could stabilize the electrostatic drift modes responsible for turbulent transport. Thus, it is possible that small, isolated magnetic islands may actually be beneficial for confinement and, for example, help to trigger transport barriers in the vicinity of rational surfaces. We shall explore this possibility in Section 2, where we calculate the impact of an isolated magnetic island chain on the stability and structure of the ion temperature gradient (ITG) mode.

The ion polarisation current plays an important role in the evolution of small scale magnetic islands. Indeed, it has been proposed as a possible threshold mechanism for neoclassical tearing modes (NTMs) in tokamaks. A complication in the theory arises from a narrow layer in the vicinity of the island separatrix where the ion polarization current provides a skin current. The contribution of this skin current to the island evolution is comparable to the contribution from other areas, but has the opposite sign. The net effect of the polarization current on tearing mode stability therefore depends on the sign of the sum of the two contributions which, in turn, requires an accurate calculation of the skin current (the contribution away from the separatrix layer is well-understood). Such a calculation is complicated by a number of effects: (1) parallel streaming competes with cross-field diffusion, so that density is not constant on a flux surface; (2) the component of electric field parallel to the magnetic field, E_{\parallel} , is unlikely to be small, and (3) finite Larmor radius effects are important. So far, only the latter effect has been taken into account in the derivation of the

polarization current: here, we treat the first and third effects self-consistently, leaving non-linear effects associated with E_{\parallel} and a final calculation of the polarization current for future work. The calculation and results are described in Section 3. We close in Section 4 with a summary.

2. ITG stability in the vicinity of a magnetic island

We introduce magnetic islands into a sheared slab model of the plasma, with magnetic field:

$$\mathbf{B} = B_0 \nabla z + \nabla \psi \times \nabla z \quad (1)$$

where

$$\psi = -\frac{B_0 x^2}{L_s} + \tilde{\psi} \cos Ky \quad (2)$$

Here, we have defined a Cartesian coordinate system (x, y, z) . The shear length, L_s , defines the rate of shear in the magnetic field. This geometry provides islands of half-width

$$w = \left(\frac{4L_s \tilde{\psi}}{B_0} \right)^{1/2} \quad (3)$$

We treat the island as a perturbation to the basic sheared slab equilibrium, in which flux surfaces are surfaces of constant x and density and temperature are functions of x only. It is convenient to define the non-adiabatic part of the distribution function, g_j , relative to the Maxwellian, $F_{Mj}(x)$:

$$f_j = \left(1 + \frac{q_j \Phi}{T_j} \right) F_{Mj} + g_j \quad (4)$$

where Φ is the electrostatic potential, q_j is the species charge and T_j is the temperature. We work in the island rest frame, in which case there is a radial electric field, E_r , and associated potential $\Phi_0 = -E_r x$. In addition there are two more contributions to the potential. One is related to the different responses of the ions and electrons to the magnetic island and is independent of time. This we denote $\bar{\Phi}$, which varies on a length scale $\sim w$ and is localised in the vicinity of the island. The second is associated with fluctuations, and is denoted $\tilde{\Phi} e^{-i\omega t}$, where ω is their complex mode frequency.

To make analytic progress, we make a number of approximations. In particular, we consider long, thin islands, such that $Kw \ll 1$; we consider fluctuations with short perpendicular wavelength compared to the island width: $k_y w \sim k_x w \ll 1$, and Larmor radius effects are assumed to be small. These approximations permit an analytic reduction of the electron and ion gyro-kinetic equation as described elsewhere [1]. Splitting the non-adiabatic part of the distribution function into the sum of a time-independent piece and a fluctuating piece, we linearise with respect to the fluctuating terms but retain non-linearities in the time-independent perturbations. This yields two types of terms in the resulting quasi-neutrality expression: ones that do not depend on time, that describe the self-consistent equilibrium in the vicinity of the island, and fluctuating terms that describe the nature of drift wave instabilities in the presence of the magnetic island. Equating the terms that do not depend on time provides an expression for the density and electrostatic potential, $\bar{\Phi}$. In particular the density is flattened across the island O-point, while a gradient is maintained near to the island X-point. The kinetic equations only predict that the density and potential are constant on the perturbed magnetic flux surfaces, but do not determine the form of the profiles across the flux surface (other than that they are related through quasi-neutrality). To do this in a fully consistent model, one must introduce a model for the cross-field transport. We avoid this

issue by choosing the form of the profile, rather than the transport model. Thus we have, for the density and potential:

$$n = n_0(0) + w \frac{dn_0}{dx} h(\chi) \quad \frac{e\Phi_0}{T_e} + \frac{e\bar{\Phi}}{T_e} = -\frac{\omega_E w}{L_n} h(\chi) \quad (5)$$

Here $n_0(x)$ is the reference density profile associated with the Maxwellian $F_{Mf}(x)$, which is assumed to have a constant gradient; $(L_n)^{-1} = -(1/n_0)(dn_0/dx)$, and the normalised equilibrium E×B drift frequency $\omega_E = -L_n e\Phi_0'/T_e$, where the prime denotes a differential with respect to x . Finally, we have introduced a flux surface function $\chi = 2x^2/w^2 - \cos Ky$. The model that we use for the profiles must satisfy the boundary condition $h(\chi) = x$ far from the island. We choose:

$$h(\chi) = \sigma \frac{\sqrt{\chi} - 1}{\sqrt{2}} \Theta(\chi - 1) \quad (6)$$

where $\sigma = |x|/x$ and $\chi = 1$ is the separatrix flux surface. The Theta-function describes the flattening of the density inside the magnetic island.

Having determined the equilibrium configuration from the time-independent terms of the quasi-neutrality equation, we now equate the fluctuating terms. Assuming a single dominant wavenumber in the y -direction, k_y , this provides the following ‘‘local’’ eigenmode equation for the structure and stability of drift waves:

$$\frac{\rho_s^2}{\tau} \frac{\partial^2 \tilde{\varphi}}{\partial x^2} + \left[\frac{L_n^2 \omega_{*e}^2}{L_s^2 \tau \rho_s^2 (\omega - \alpha_d S)^2} x^2 - \left[\frac{(\omega - \alpha_d S) - (\omega_{*e} - \alpha_n S / \omega_E)}{(\omega - \alpha_d S) \tau + (1 + \eta_i)(\omega_{*e} - \alpha_n S / \omega_E)} + b \tau^{-1} \right] \right] \tilde{\varphi} = 0 \quad (7)$$

We have defined the sound speed Larmor radius, ρ_s , the electron diamagnetic frequency, ω_{*e} , $b = (k_y \rho_s)^2$, $\tau = T_e/T_i$ and $\eta_i = L_n/L_T$ is the ratio of ion density and temperature gradient scale lengths. The effects of the profile modification are captured in the variable S , where:

$$S = \omega_{*e} \omega_E \left(1 - w \frac{\partial h}{\partial x} \right) \quad (8)$$

which has a weak dependence on y and a somewhat stronger dependence on x (on a length scale $\sim w$). Comparing with the standard expression for drift waves in a sheared slab, we see that there are two modifications due to the island. First are the terms labelled with α_d . These represent the effect of the sheared E×B flow around the island due to the potential $\bar{\Phi}$. Second are the terms labelled α_n , which represent the modifications to the density profile (and hence

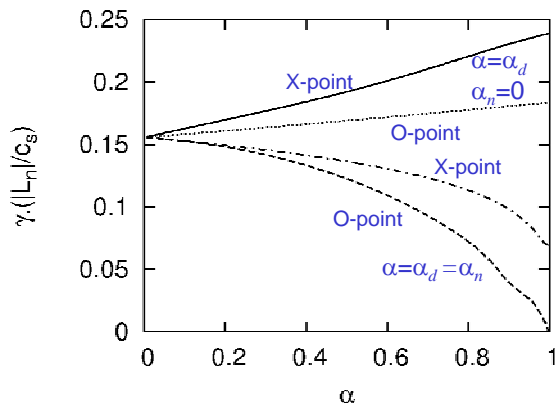


Figure 1: Growth rate as the α parameters are increased from 0 (no island) to 1 (full island). The full and dotted curves show the impact of the sheared flow profile, while the dashed curves include both flow and density profile modifications.

ω_{*e}). The α parameters are introduced as a convenient way to map smoothly from the situation with no island ($\alpha_{n,d} = 0$) to the full island physics ($\alpha_{n,d} = 1$).

Focussing on the ion temperature gradient (ITG) mode, we solve Eq (7) in the local (in y) approximation to explore how profile modifications affect stability. The results are shown in Fig 1 for $\eta_i = 100$, $\tau = 25$, $w/\rho_s = 5$, $L_s/L_n = 5$, $\omega_E = -0.5$. This figure shows the local growth rate at two values of y , corresponding to the island X-point and O-point. Referring to Fig 1, consider first the full and dotted curves. For these, we fix $\alpha_n = 0$ and vary α_d to illustrate the impact of the flow shear without the modifications to the density

profile. It can be seen that the flow shear has a destabilising effect, which is consistent with the results of Wang et al [2] for the level of flow shear that we calculate here. The density profile modifications, on the other hand, are strongly stabilising, particularly at the value of y corresponding to the island O-point.

Such a local stability analysis is rather crude: it provides only a qualitative indication of the growth rate, and there is no information about the mode structure in the y -direction. To explore this more rigorously, we return to the full 2-D equation describing the drift mode stability by replacing $k_y \rightarrow i\partial/\partial y$ in Eq (7) (in a form where all k_y factors appear in the numerator of each term). Employing Fourier modes in the y -direction, and finite differences in the x -direction, we solve the full 2-D system, to derive the mode structure illustrated in Fig 2. We note two important features: (1) from Fig 2a, we see that the mode is not localised at the position of maximum instability (ie the X-point), as one might naively expect; (2) from Fig 2b, a number of k_y values are coupled, but the frequency spectrum is relatively narrow.

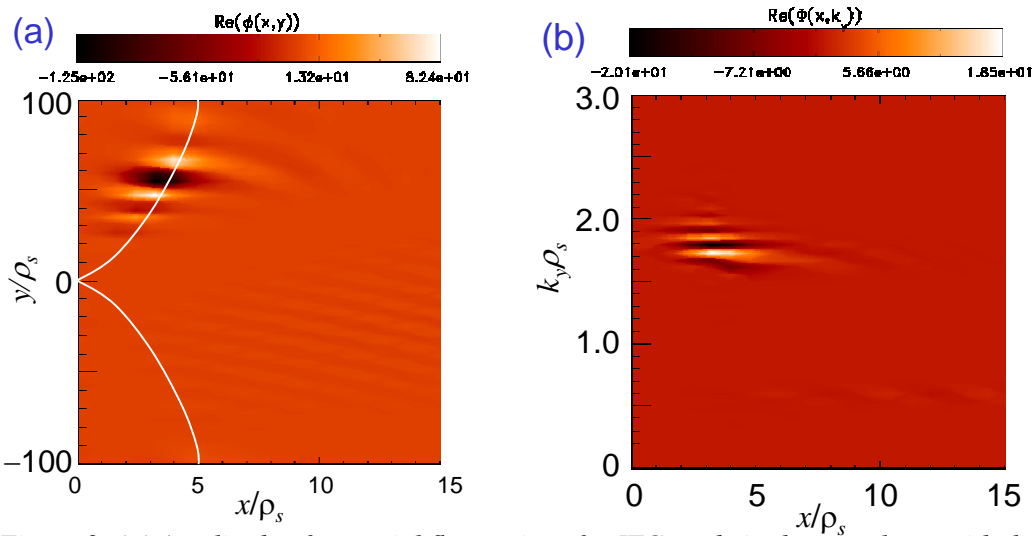


Figure 2: (a) Amplitude of potential fluctuations for ITG mode in the x - y plane, with the island separatrix marked in white; (b) frequency spectrum for this mode as a function of x .

To understand why the mode is not localised around a position of maximum instability, one can develop a WKB solution and, by assuming a localised solution exists (in y), it is possible to develop a self-consistent ordering as in [1], for example. There, we found that to leading order the stability is determined from Eq (7), but with a specific *complex* $k_y = k_0$ that satisfies $d\omega/dk_y = 0$. The imaginary part of k_0 then determines the shift in the y -position of the mode relative to the X-point (ie the maximally unstable position). The theory is complicated by the 2-D nature of the shear function, S , so here we shall illustrate the essential features with a simple model. This model involves setting $\alpha_n = \alpha_d = 0$ in Eq (7), and introducing a y -dependence through a sinusoidally varying η_i . Eq (7) can be obtained by assuming an eikonal form for the solution of the full 2D equation $\sim \exp(-i \int k_y dy)$. Let us define an arbitrary reference wavenumber, k_0 , and introduce a normalised wavenumber $k = k_y/k_0$, together with $\Omega = \omega/\omega_{*e}$, where $\omega_{*e} = k_0 \rho_s c_s / L_n$. In fact, it is convenient to choose $k_0 \rho_s = 1$. Eq (7) then becomes

$$\rho_s^2 \frac{\partial^2 \tilde{\phi}}{\partial x^2} + \left[\frac{\sigma^2 k^2}{\rho_s^2 \Omega^2} x^2 + \left(\frac{\Omega - k}{\Omega + \eta} \right) + k^2 \right] \tilde{\phi} = 0 \quad (8)$$

We have introduced the new parameter $\eta = (1 + \eta_i)/\tau$, which contains the sinusoidal y -dependence:

$$\eta = (1 + \eta_i)/\tau = \eta_0 (1 + \varepsilon \cos Ky)$$

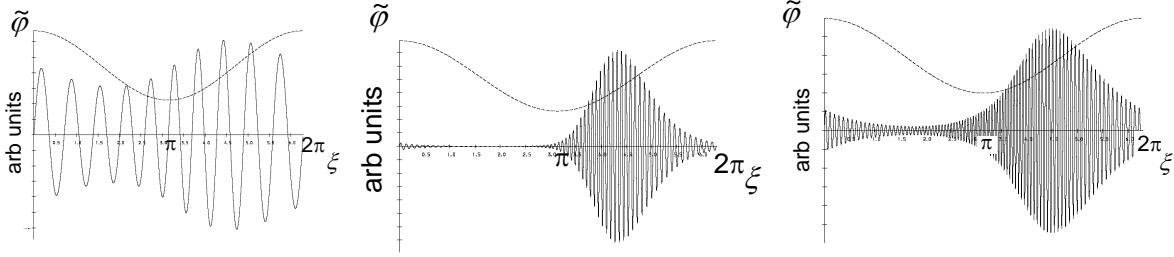


Figure 3: Numerical solution of Eq (9) for three cases, from left to right $k_y \rho_s = 0.02$, $k_y \rho_s = 0.14$, and $k_y \rho_s = 0.18$ (k_y is the wavenumber of the fine-scale oscillation). The dashed curve shows the form of η . Parameters are $\rho_* = 0.002$, $\eta_0 = 2$, $\varepsilon = 0.5$ and $\sigma = 0.5$.

The advantage of the model Eq (8) is that it has an analytic solution, and yields a cubic equation for k for the eigenvalue condition. Transforming this eigenvalue equation back to real space, and introducing a dimensionless variable, $\xi = Ky$, yields:

$$\left[i\eta\rho_*^3 \frac{\partial^3}{\partial \xi^3} - \rho_*^2 \left(\Omega \mp \frac{i\sigma\eta}{\Omega} \right) \frac{\partial^2}{\partial \xi^2} + i\rho_* (1 \mp i\sigma) \frac{\partial}{\partial \xi} + \Omega \right] \tilde{\varphi} = 0 \quad (9)$$

where $\rho_* = K\rho_s \ll 1$. The sign is chosen to maximise the growth rate. We can make analytic progress by adopting the WKB procedure of [1] (as described above). Before we consider that, let us first solve Eq (9) numerically. Figure 3 shows three forms of solution for $\tilde{\varphi}$, with periodic boundary conditions $\tilde{\varphi}(\xi) = \tilde{\varphi}(\xi + 2\pi)$. In the first, we have chosen a mode with low $k_y \rho_s = 0.02$ with relatively few nodes in the periodic domain. The mode is similar in structure to the standard sheared slab mode, with only a slight modulation of the amplitude. The second solution is more interesting, with a higher value of $k_y \rho_s = 0.14$. Two important points are: (1) the mode is now localised in ξ (or y) and (2) it is *not* localised about the position of maximum η . Finally, as we proceed to still higher $k_y \rho_s = 0.18$ we find that the mode again becomes more extended in nature. As we increase $k_y \rho_s$ still further, the mode again becomes slab-like in nature, with a relatively weak modulation in the amplitude.

To understand the intermediate, localised regime, let us develop an analytic WKB solution to Eq (9) in the limit $k_y \rho_s \sim 1$ and $\rho_* \ll 1$. Recalling $k = k_y \rho_s$, we write a solution to Eq (9) in the form $\tilde{\varphi} = \exp(-i \int k d\xi / \rho_*) f(\xi)$ and expand in ρ_* : $f = f_0 + \rho_* f_1 + \dots$; $\Omega = \Omega_0 + \rho_*^2 \delta\Omega + \dots$. We shall find that this ordering is valid provided the mode maximum is not shifted too far from the point at which $\Omega_0(\xi)$ is maximum. To leading order we find:

$$F(\Omega, k, \xi) f_0 = \left[-\eta k^3 + \left(\Omega_0 \mp \frac{i\sigma\eta}{\Omega_0} \right) k^2 + (1 \mp i\sigma)k + \Omega_0 \right] f_0 = 0 \quad (10)$$

yielding an expression for $\Omega_0(k, \xi)$. The next order equation yields:

$$iF_k \frac{\partial f_0}{\partial \xi} + F f_1 = 0 \quad F_k \equiv \left. \frac{\partial F}{\partial k} \right|_{\Omega} \quad (11)$$

As $F=0$ from Eq (10), clearly we must have $F_k=0$, and this equation combined with Eq (10) determines both Ω_0 and k . Indeed, the condition $F_k=0$ is equivalent to $\partial\Omega_0/\partial k=0$ that we deduced for the general case in ref [1]. We find that k is complex. Proceeding to second order, with $F_k=0$ and $F=0$, we have:

$$F_{kk} \rho_*^2 \frac{\partial^2 f_0}{\partial \xi^2} = F_{\Omega} [\Omega - \Omega_0(\xi)] f_0 \quad (12)$$

which, in general, is a Mathieu-type of equation because of the periodic nature of Ω_0 . However, the sinusoidal variation of Ω_0 may provide a “potential well” and, if this is sufficiently deep, localised solutions exist. These confined modes arrange themselves so that f_0 is localised around a stationary point of Ω_0 (eg near the point of maximum instability). In particular, Taylor expanding $\Omega_0(\xi)$ about this point yields the solution:

$$f_0 = \exp \left[\pm \frac{i}{2} \left(-\frac{F_{\Omega}}{F_{kk}} \Omega_{\xi\xi\xi} \right)^{1/2} \frac{(\xi - \xi_0)^2}{\rho_*} \right] \quad (13)$$

where $\xi = \xi_0$ is the position of maximum growth rate. This solution demonstrates that the envelope function is localised on a length scale $\sim \sqrt{\rho_*}$, which is intermediate between the fast variation scale and the “equilibrium” scale represented by the variation in η . Note, however, although f_0 is localised around the position of maximum instability, $\tilde{\varphi}$ is not. Recalling the form of the full solution above Eq (10), we find that $\tilde{\varphi}$ is localised around a point $\xi = \xi_1$, where

$$\xi_1 = \xi_0 + \text{Im}(k) / \text{Re} \left[\frac{i}{2} \left(-\frac{F_{\Omega}}{F_{kk}} \Omega_{\xi\xi\xi} \right)^{1/2} \right] \quad (14)$$

If $\text{Im}(k)$ ($\equiv \text{Im}(k_y \rho_s)$) is non-zero, this represents a shift in the point of localisation, away from the point of maximum instability, as seen in the numerical solutions of Fig 3. However, the numerical solutions also demonstrate that if one considers modes with higher k ($> \sim 1$) the eigenfunction begins to “tunnel” out of the well and is not localised. The theory described here shows that as $\text{Im}(k)$ increases, the shift in the point of localisation becomes a significant fraction of the distance between island X-points. The ordering we assumed then breaks down because f_0 only varies slowly (i.e. $\sim \sqrt{\rho_*}$) compared to the eikonal close to where $\xi = \xi_0$. To treat this higher $\text{Im}(k)$ regime, we therefore need a more complete analysis of the Mathieu equation, which has strong mathematical similarities with the treatment of rotation shear effects on drift waves [3]; this is work in progress.

3. The impact of finite radial diffusion on the polarisation current in magnetic islands

In the previous section, specifically Eq (5), we found that the density is constant on the perturbed flux surfaces of the magnetic island geometry. However, from Eq (6) we see that the density gradient is not continuous at the separatrix ($\chi=1$) and this has implications for the polarisation current in that vicinity, as noted in [4]. In particular, the discontinuity generates a skin current at the separatrix which opposes the contribution to the polarisation current from elsewhere. As a result, whether the polarisation current is stabilising or destabilising depends on a subtle balance between these two components. Three effects can be identified with the “separatrix layer”: (1) finite ion Larmor radius effects are important; (2) the density is no longer a flux surface quantity there, and (3) non-linearities involving the component of electric field parallel to the magnetic field lines are likely to be important. Only the first point has been addressed so far [5]. Here, we extend the theory to retain both the first and second effects, and treat the effect of the parallel electric field linearly. This requires us to retain cross-field diffusion in the vicinity of the separatrix.

Assuming that the potential is smoothed on ion Larmor radius length scales, and that the region over which diffusion is important is more narrow than the ion Larmor radius, the electron response is described by the equation:

$$v_{\parallel} \nabla_{\parallel} f_e = D \frac{\partial^2 f_e}{\partial x^2} + \nu (f_e - n(\chi) F_M) \quad (15)$$

where the integral over velocity space of the Maxwellian F_M gives 1. [We neglect the parallel electric field in our description of the formalism, but it is retained through an adiabatic term in the code.] Neglecting the collisional term in the separatrix layer, a procedure for solving this equation is described in [6], employing a Wiener-Hopf formalism. Outside the separatrix region we know two things about the distribution function: (1) it is constant on flux surfaces and (2) it is a Maxwellian. These provide boundary conditions to the layer solution. To impose these boundary conditions, we follow [6] and identify a short-scale radial variable

$$r = \frac{\sqrt{\pi}}{2} \left(\frac{Kw^3u}{L_s D} \right)^{1/2} \int_1^\kappa \frac{\kappa^{1/2}}{E(\kappa^{-2})} d\kappa \quad \kappa^2 = \frac{\chi+1}{2} \quad (16)$$

where $u=|v_{\parallel}|$ and note that $\kappa=1$ at the separatrix. Taking the limit $r \rightarrow \infty$, takes us out of the separatrix layer to where we must match to the flux surface Maxwellian. Specifically [6],

$$\lim_{r \rightarrow \infty} f_e = c_1 [r + 0.855] = c_1 \left[\left(\frac{\pi K w^3 u}{L_s D} \right)^{1/2} \frac{\chi-1}{8} + 0.855 \right] \quad (17)$$

where the unknown quantity c_1 is a function of velocity. A problem is immediately apparent: while this is indeed a flux quantity, the presence of u means that it cannot be matched to a Maxwellian. To resolve the situation we must introduce an intermediate matching region where collisions are important and the full Eq (15) must be solved. We employ an expansion where the dominant term is the parallel flow, to derive the solution in the matching region:

$$f_e = n(\chi)F_M + A(v)g(\chi) \quad \text{where} \quad \frac{d}{d\chi} \left(Q \frac{dg}{d\chi} \right) = 2 \frac{dQ}{d\chi} \frac{w^2 v}{8D} g \quad (18)$$

and Q is a known function of χ involving elliptic integrals. Because we have now defined a transport model, this provides a constraint for $h(\chi)$ and we cannot use the form given in Eq (6). Instead, we derive

$$n(\chi) = \frac{1}{2\sqrt{2}} \frac{w}{L_n} \int_1^\chi \frac{d\chi}{Q} + a \quad (19)$$

We solve Eq (18) for g numerically with the boundary condition that $g \rightarrow 0$ far from the island. Equations (17) and (18) can be used to match the forms for f_e and its derivatives with respect to χ , to provide two equations for the 3 unknown quantities a , c_1 and $A(v)$. The final constraint results from the condition that the integral of A over velocity space must be zero (as $n(\chi) = \int f_e d^3v$). A numerical solution in the separatrix layer using the formalism of [6], together with the above matching conditions, provides the electron distribution function. The result is shown as a function of v_{\parallel} in Fig 4a, which clearly illustrates the non-Maxwellian nature near

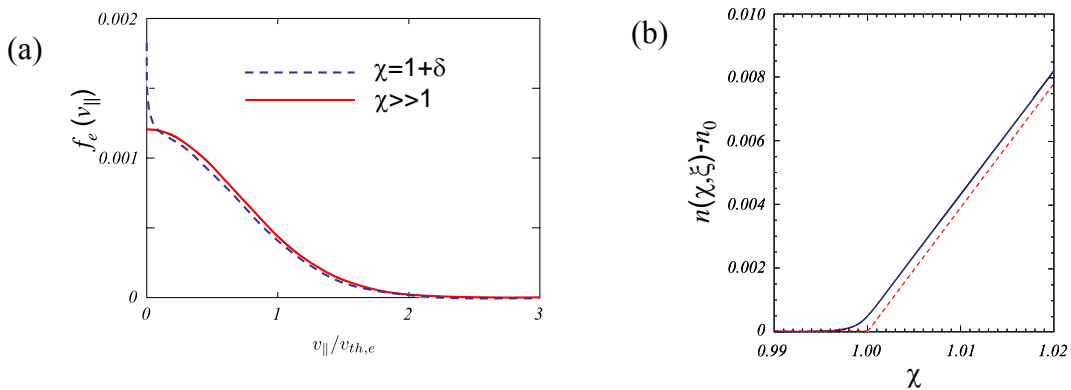


Figure 4: (a) Electron distribution function near to the separatrix (dashed curve) and far from it (full curve). (b) Density profile across the island O-point in the vicinity of the separatrix with (full) and without (dashed) diffusion effects.

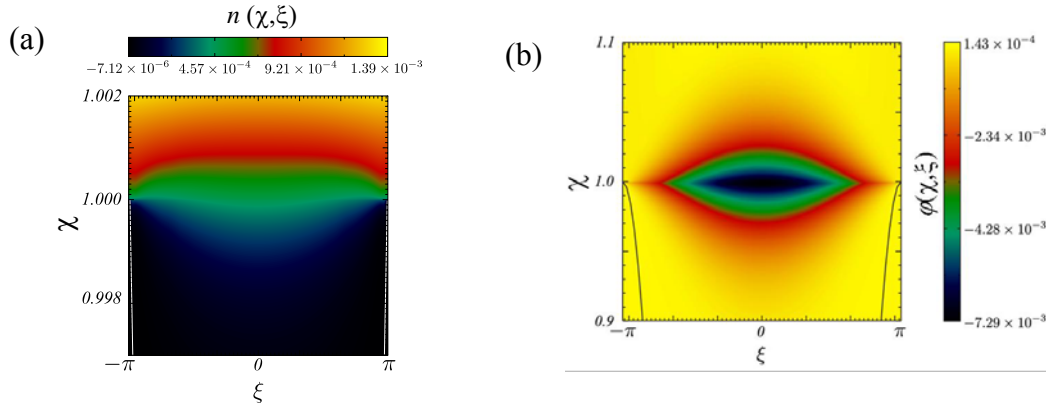


Figure 5: 2-D colour contour plots of the density (a) and potential (b), showing that neither are flux surface quantities in the separatrix layer.

the island separatrix at $\chi=1+\delta$ ($\delta \ll 1$). Integrating this over velocity space provides the electron density which is smoothed through the separatrix layer (Fig 4b). One consequence of the diffusion is that the density is no longer a flux surface quantity in the vicinity of the island separatrix. This is illustrated by the colour contour plot of Fig 5.

The ultimate aim of this work is to calculate the impact of the ion polarisation current on the evolution of tearing modes. This requires a calculation of the electrostatic potential, $\bar{\Phi}$. To derive this, we require an expression for the ion response to $\bar{\Phi}$, which is evaluated using the ion gyrokinetic equation, retaining full FLR effects (recall that the separatrix layer where transport is important is assumed to be more narrow than the ion Larmor radius). Quasi-neutrality then yields a solution for $\bar{\Phi}$ (see Fig 5(b)). Although the procedure is a little more complicated by the presence of the separatrix layer, the polarisation current can then be derived from $\bar{\Phi}$. This is work in progress.

4. Summary

In this paper we have described two pieces of work related to the interaction between transport and the reconnection process. In the first, we showed how a tearing mode island can substantially affect both the structure and growth rates of the linear ITG mode, suggesting that turbulent transport processes are significantly modified in the vicinity of a magnetic island. In the second study, we described how cross-field diffusion is important close to the island separatrix, where it resolves a discontinuity in the density gradient. The forms for the density and potential have been evaluated, consistent with the constraint of quasi-neutrality. These are necessary ingredients in a complete calculation of the impact of ion polarisation current on tearing mode evolution, which we are working towards.

Acknowledgement This work was funded jointly by the United Kingdom Engineering and Physical Sciences Research Council and by the European Communities under the contract of Association between EURATOM and UKAEA. The views and opinions expressed herein do not necessarily reflect those of the European Commission.

REFERENCES

- [1] M. James, et al Proceedings of the 35th EPS Conference on Plasma Physics and Controlled Fusion, Crete (2008)
- [2] X.-H. Wang, P.H.Diamond and M.N. Rosenbluth Phys Fluids B4 (1992) 2402
- [3] J W Connor and T J Martin, Plasma Phys Contr Fusion **49** (2007) 1497
- [4] F.L. Waelbroeck and R. Fitzpatrick, Phys Rev Lett **78** (1997) 1703
- [5] F.L. Waelbroeck, J.W. Connor and H.R. Wilson, Phys Rev Lett **87** (2001) 215003
- [6] R.D. Hazeltine, P. Helander and P.J. Catto, Phys Plasmas **4** (1997) 2920